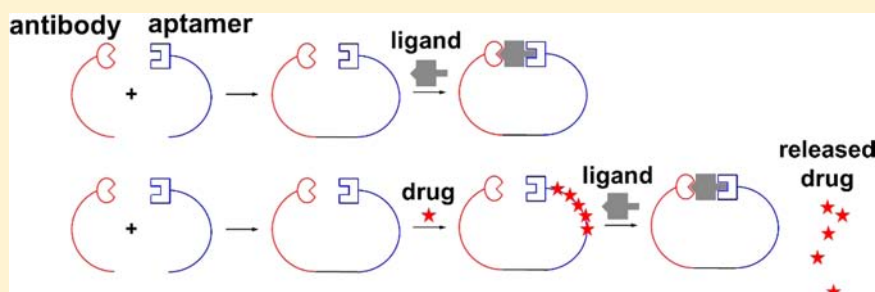


# Improved Ligand Binding by Antibody–Aptamer Pincers

Sungmuk Kang and Sang Soo Hah\*

Department of Chemistry and Research Institute for Basic Sciences, Kyung Hee University, 1 Hoegi-dong Dongdaemun-gu, Seoul 131-701, South Korea

**S** Supporting Information



**ABSTRACT:** To increase the affinities of antibodies or aptamers for their targets, we designed antibody–aptamer pincers (AAPs) or heterodimers for thrombin or human epidermal growth factor 2 (HER2) as a model system. For this purpose, we first conjugated a 15-mer or 29-mer anti-thrombin aptamer, which are well-known to bind to thrombin in two specific epitopes, with an anti-thrombin antibody to enable each binding part of the AAP to simultaneously recognize a different part of the thrombin molecule. The AAP comprising a 15-mer aptamer and an anti-thrombin antibody has an apparent dissociation constant ( $K_d^{AAP}$ ) value of 567 pM, and this value is approximately 1/100 of that of the antibody alone or 1/35 of that of the aptamer monomer alone. The AAP comprising a 29-mer aptamer and an anti-thrombin antibody has a much lower  $K_d^{AAP}$  value than that of 15-mer aptamer-conjugated antibody. Furthermore, this concept of the AAP system was employed to HER2-targeted drug delivery system (DDS) based on both antibody and drug-loaded aptamer. Anti-HER2 aptamer was conjugated with anti-HER2 antibody and loaded with doxorubicin, and the resulting AAP-HER2-Dox was found to have approximately 3- and 6-fold higher cytotoxicity than drug alone and antibody alone, respectively. Therefore, this novel AAP system constructed by conjugation of the antibody with the aptamer can effectively improve the affinities of the resulting AAPs for their target molecules and the drug-loaded AAP system can possibly serve as a platform for targeted DDS against many malignancies.

## INTRODUCTION

It has been reported that antibody dimerization, the components of which simultaneously recognize adjacent and nonoverlapping epitopes, can enhance the receptor binding.<sup>1–3</sup> The reports demonstrate that by connecting two antibodies that recognize different parts of the target molecule, the  $K_d$  value of the resulting antibody dimer can be lowered, because the  $k_{on}$  value increases and the  $k_{off}$  value decreases when binding together to two recognition sites of the same target, in comparison with the  $K_d$  value of either of the two antibodies.<sup>1–3</sup> Thus, the affinity of the antibody dimer can be increased by connecting together two antibodies that have nonoverlapping epitopes.

In consideration of the advantages of using aptamers instead of antibodies in clinical diagnosis, it would be highly advantageous to replace antibodies with aptamers as molecular recognition elements. Aptamers are a special class of nucleic acids that can specifically bind, with high affinity, to a wide array of target molecules.<sup>4–9</sup> They have originated from large random-sequence nucleic acid libraries via an in vitro evolution process called SELEX (Systematic Evolution of Ligands by EXponential enrichment). Emerging as successful alternatives to antibodies, a wide range of DNA-, RNA-, and PNA (peptide

nucleic acid)-based aptamers have been reported to bind with the dissociation constants ranging from nanomolar to picomolar level, specifically to metal ions,<sup>10–12</sup> small molecules,<sup>13,14</sup> proteins,<sup>6–9</sup> and even entire cells.<sup>15</sup> Notably, aptamers screened via in vitro process against a synthetic library have a number of unique features which make them a more effective choice than antibodies. First, the limit of having to use cell lines or animals, as is necessary for antibodies, can be overcome. Aptamers, once selected, can undergo subsequent amplification through polymerase chain reaction or transcription to produce a large quantity with high purity. Second, the simple chemical structure of aptamer makes it amenable to further modifications with functional groups based on the experimental purposes. Finally, aptamers are more stable than antibodies, allowing them to be suitable in applications requiring harsh conditions (e.g., high temperature or extreme pH).

Of importance, Kim et al. recently explored the design of bivalent nucleic acid ligands by using thrombin and its aptamers

**Received:** March 10, 2014

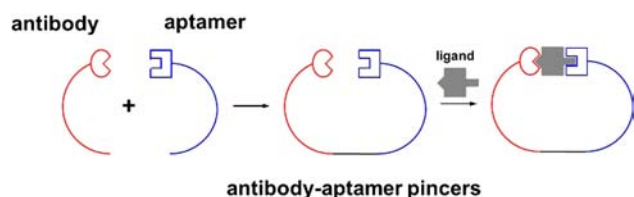
**Revised:** July 9, 2014

**Published:** July 10, 2014

as the model by which to evaluate its functions,<sup>16</sup> and Hasegawa et al. also reported in the same year that an aptamer heterodimer for thrombin and a homodimer for vascular endothelial growth factor (a homodimeric protein) could exhibit increased affinities for the targets, respectively.<sup>17</sup> In contrast to the antibody dimerization, however, only a 10-fold lower  $K_d$  value of the monomers, of which the heterodimer for thrombin was composed, could be achieved. This is attributed presumably to the higher  $k_{\text{off}}$  value of the aptamer dimer than that of the antibody dimer. Therefore, to more effectively increase the affinities of antibodies or aptamers for their targets, we reasoned to design antibody–aptamer pincers (AAPs) or heterodimers for a target molecule, such as thrombin, as a model system, because aptamers could be easily modified with various molecules including with antibodies in comparison to the antibody dimerization and because aptamers are still interesting candidates as alternatives to antibodies which can be introduced to the antibody-linked pincers or heterodimers from the flexibility point of view. Moreover, we hypothesized that this AAP system might result in bivalent ligand-mediated higher binding affinity as well as antibody-mediated higher specificity than the simple bivalent aptamers, because only a few aptamers are reported to date to exhibit higher specificity than antibodies.<sup>4–9</sup> This system was also expected to allow us to make use of aptamers as loading docks for intercalating drugs, such as doxorubicin (Dox), for new targeted drug delivery systems (DDSs) or to enable us to introduce functional groups to aptamers, because the simple chemical structure of aptamers makes them amenable to further modifications with functional groups depending on the experimental purposes.

Scheme 1 illustrates the simplified principle of our AAP system. Anti-thrombin aptamers were first chosen in the

**Scheme 1. Schematic Illustration of the Antibody–Aptamer Pincer (AAP) or Heterodimer System in the Present Study**



present study to be used as an antibody counterpart in the AAP system, because one of the most commonly studied proteins for molecular targets in aptamer-based assays is thrombin, the last enzyme protease involved in the coagulant cascade, which converts fibrinogen to insoluble fibrin that forms the fibrin gel.<sup>18</sup> Since the DNA aptamers against thrombin were investigated,<sup>19</sup> it has been known that they consist of two G-quartet conformations and bind to thrombin in two specific epitopes (15-mer DNA aptamer, also known as HD-1, which binds fibrinogen-binding exosite I of thrombin via a T-loop; 29-mer DNA aptamer, referred to as HD-22, which binds to heparin-binding exosite II of thrombin).<sup>20,21</sup> This property has allowed for the development of aptamer-based sandwich assays for the detection of thrombin with higher specificity than direct immunoassays.<sup>22</sup> Thus, a 15-mer or 29-mer anti-thrombin aptamer was conjugated with an anti-thrombin antibody (see the Supporting Information for detailed experimental conditions), resulting in formation of AAP-15 or AAP-29, in order to enable each binding part of the AAP to simultaneously recognize a different part of the thrombin molecule. According

to the literature, anti-thrombin antibody (monoclonal antibody F-1), 15-mer and 29-mer DNA aptamers have  $K_d^{\text{app}}$  values for thrombin of approximately 50 nM, 20.2 nM, and 3.5 nM, respectively.<sup>20,21,23</sup>

## RESULTS AND DISCUSSION

The affinities of the designed AAPs (Figure S1, Supporting Information) for dye-labeled proteins (Figure S2) were investigated by dialysis. Figure 1A shows that the AAP

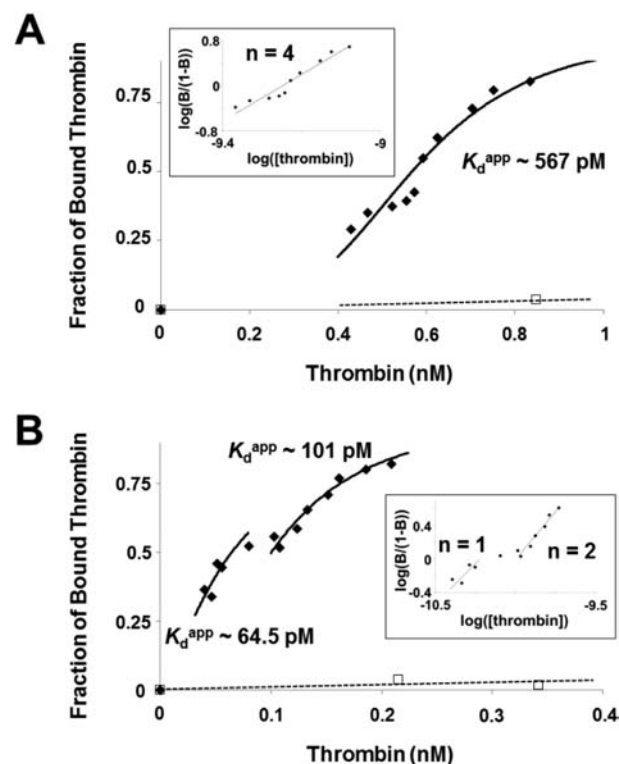


**Figure 1.** Thrombin binding characteristics of anti-thrombin antibody conjugated with anti-thrombin aptamer. (A) FAM-labeled thrombin (filled) or bovine serum albumin (BSA) (empty) binding of anti-thrombin antibody conjugated with anti-thrombin 15-mer aptamer (AAP-15). Inset: Hill plot. (B) FAM-labeled thrombin (filled) or BSA (empty) binding of anti-thrombin antibody conjugated with anti-thrombin 29-mer aptamer (AAP-29). Inset: Hill plot.

comprising a 15-mer aptamer and an anti-thrombin antibody (AAP-15) has an apparent dissociation constant ( $K_d^{\text{app}}$ ) value of 567 pM for thrombin, and this value is approximately 1/100 of that of the antibody alone or 1/35 of that of the aptamer monomer alone. A Hill plot reveals positive cooperativity (Hill  $n$  value  $\sim 4$ ). Very interestingly, the AAP comprising a 29-mer aptamer and an anti-thrombin antibody (AAP-29) has a much lower  $K_d^{\text{app}}$  value than that of 15-mer aptamer-conjugated antibody (Figure 1B), probably due to the higher binding affinity between a 29-mer aptamer and thrombin than between a 15-mer aptamer and thrombin. The data in Figure 1B indicate that AAP-29 binds to thrombin in a biphasic mode with a lower  $K_d^{\text{app}}$  value of 64.5 pM and with a higher  $K_d^{\text{app}}$  value of 101 pM, of which the Hill plot suggests cooperativity of the second binding phase of thrombin binding to AAP-29 (Hill  $n$  value  $\sim 2$ ). Importantly, many AAP systems are expected to be newly designed, as long as aptamers that are able to bind different epitopes of a given target are known, as clearly demonstrated in this study.

Inspired by the exciting results, the AAP system was employed to HER2-targeted DDSs based on both antibody and drug-loaded aptamer, because several targeted DDSs are still among the hot topics discussed in the field of biopharmaceutical development, toxicology, immunology, and clinical pharmacy.<sup>24</sup>

To address this issue, an anti-HER2 aptamer was chosen,<sup>25</sup> and conjugated with an anti-HER2 antibody (monoclonal antibody N12) to form AAP-HER2 (Supporting Information Figure S3), followed by formulation with Dox intercalated into the DNA structure of the anti-HER2 aptamer (Dox-loaded AAP-HER2 or AAP-HER2-Dox). According to the literature, the anti-HER2 aptamer has two recognition sites, able to bind to an epitope peptide of HER2 with a  $K_d$  of 18.9 nM or to the extracellular domain of HER2 protein with a  $K_d$  of 316 nM,<sup>25</sup> while the epitope for the anti-HER2 antibody is located to C531-A586 and the anti-HER2 antibody alone can inhibit HER2-positive tumor cell proliferation.<sup>26</sup> Thus, it was expected that each of the two binding parts of the AAP-HER2 or AAP-HER2-Dox could recognize a different part of the HER2 molecule, and that HER2-containing tumor cell proliferation could be specifically inhibited by both the anti-HER2 antibody and Dox.<sup>25,26</sup>

The formation of the AAP-HER2-Dox complex was evaluated, based on the fact that the fluorescent Dox can be quenched after intercalation into DNA duplex structure.<sup>25</sup> Supporting Information Figure S4 clearly demonstrates that anti-HER2 aptamer could be loaded with Dox and the ratio of 1:10 between aptamer and Dox would result in the highest fluorescence emission difference. Thus, the ratio of 1:10 for AAP-HER2-Dox was used for the following viability experiments. It is interesting to note that Dox can be intercalated more efficiently into anti-HER2 aptamer than into anti-thrombin 29-mer aptamer or single-stranded DNA 1 (ssDNA1, a scrambled DNA sequence as the negative control) (Supporting Information Figure S4D).

Next, in order to verify whether the presence of HER2 can alter the folding state of Dox-loaded anti-HER2 aptamer and affect the drug release, fluorescence spectra assays were performed (Supporting Information Figure S5). The results elucidate that the binding event between Dox-loaded anti-HER2 aptamer and HER2 epitope changes the folding of Dox-loaded anti-HER2 aptamer and thus induces the intercalated Dox to be released. The data also indicate that the apparent dissociation constant ( $K_d^{app}$ ) between Dox-loaded anti-HER2 aptamer and HER2 epitope is approximately 50 nM, in comparison with the reported value of  $K_d$  (18.9 nM) between anti-HER2 aptamer and HER2,<sup>25</sup> indirectly suggesting that Dox intercalation might induce some alteration of the folding state of anti-HER2 aptamer.

The cytotoxicity of AAP-HER2-Dox was measured via the standard MTT assay, in order to evaluate whether AAP-HER2-Dox could modulate the in vitro growth of three human breast cancer cell lines with different HER2 expression levels. Figure 2A shows that AAP-HER2-Dox is able to inhibit cell viability at different degrees after 24 h. The obtained  $IC_{50}$  values of AAP-HER2-Dox for SK-BR-3, MDA-MB-453, and MCF-7 cells were 15.5, 35.0, and 83.4 nM, respectively. The data are strongly correlated with the cellular expression levels of HER2,<sup>8</sup> suggesting that AAP-HER2-Dox can discern target and nontarget cells and that the complex can thus be used for specific DDS for HER2-overexpressed cancer cells.

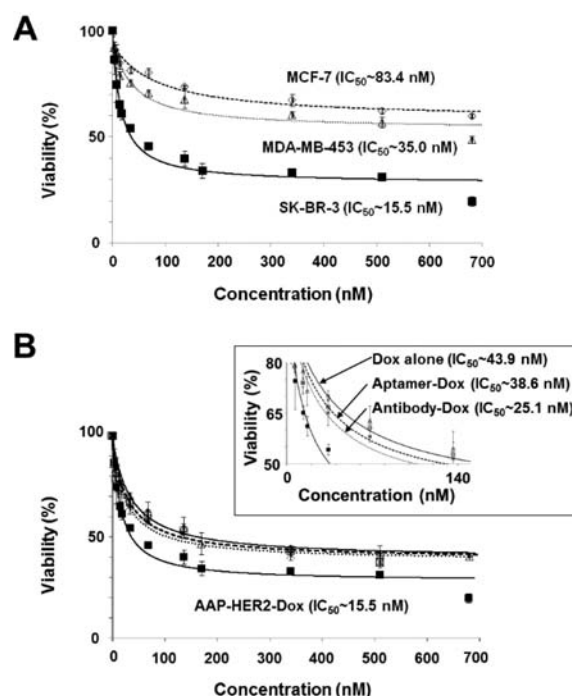


**Figure 2.** (A) Effects of an anti-HER2 AAP system loaded with Dox (AAP-HER2-Dox) on cell viability of SK-BR-3, MDA-MB-453, and MCF-7 cell lines. (B) Dose-dependent viability of SK-BR-3 in the presence of AAP-HER2-Dox, anti-HER2 antibody mixed with Dox (Antibody-Dox), anti-HER2 aptamer loaded with Dox (Aptamer-Dox), or Dox alone. Cells were exposed to the given materials (0–680 nM in terms of the total amounts of loaded and free Dox). The values represent means  $\pm$  SD of three cultures from triplicate-independent experiments. The experimental data were transformed to dose-response curves using nonlinear regression analysis (SigmaPlot) to obtain the theoretical curves and to calculate the corresponding  $IC_{50}$  values. Inset: Enlarged graph to distinguish the curves better.

SK-BR-3 cells with the highest expression levels of HER2 on the plasma membrane were then chosen and exposed to Dox-mixed anti-HER2 antibody (Antibody-Dox) or to Dox-loaded anti-HER2 aptamer (Aptamer-Dox) in comparison to that of AAP-HER2-Dox. Figure 2B reveals that the cytotoxic effects of AAP-HER2-Dox are drastically different in a dose-response manner from Antibody-Dox, Aptamer-Dox, or Dox alone, indicating that the AAP-HER2-Dox exhibits the highest cytotoxicity in SK-BR-3 cells among the four materials. The  $IC_{50}$  values of AAP-HER2-Dox, Antibody-Dox, Aptamer-Dox, and Dox were estimated to be 15.5, 25.1, 38.6, and 43.9 nM for SK-BR-3, respectively, suggesting that AAP-HER2-Dox is approximately 3-fold more cytotoxic than Dox.

Interestingly, although the anti-HER2 aptamer alone produced no cytotoxicity in SK-BR-3 cells (Supporting Information Figure S6), Aptamer-Dox was cytotoxic even compared with Dox, which is consistent with the literature.<sup>25</sup> The cytotoxicity of Antibody-Dox, on the other hand, is similar to or between that of Aptamer-Dox and Dox. This result is also interesting in consideration that Dox cannot be loaded into the antibody (Supporting Information Figure S4) and that the anti-HER2 antibody alone can inhibit HER2-positive tumor cell proliferation.<sup>26</sup> To further investigate whether Aptamer-Dox and Antibody-Dox indeed enhance the cancer killing effect of Dox, the cytotoxicity of Aptamer-Dox and Antibody-Dox in comparison with that of Dox alone was measured as a function



of the incubation time, and our data in Figure 3 and Supporting Information Figure S7 reveal that the presence of anti-HER2 aptamer or antibody indeed enhances the Dox killing effect, although it is relatively small.

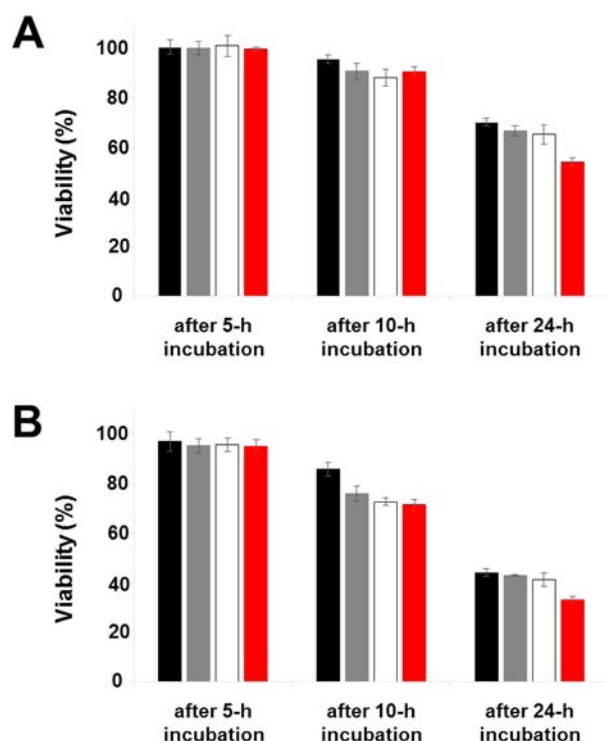


**Figure 3.** Incubation time-dependent viability of SK-BR-3 in the presence of Dox alone (black), Aptamer-Dox (gray), Antibody-Dox (white), and AAP-HER2-Dox (red), respectively. Cells were exposed to the given materials (34 nM (A) and 340 nM (B), in terms of the total amounts of loaded and free Dox). The values represent means  $\pm$  SD of three cultures in triplicate. The results indicate that Aptamer-Dox and Antibody-Dox show better cancer killing than Dox alone, respectively, even for shorter time periods, suggesting that the presence of anti-HER2 aptamer or antibody may enhance Dox killing effect.

In addition, control experiments using three negative controls of Dox-loaded anti-thrombin 29-mer aptamer conjugated with anti-HER2 antibody, Dox-loaded ssDNA1 (a scramble DNA sequence) conjugated with anti-HER2 antibody, and Dox-loaded anti-HER2 aptamer conjugated with anti-HER2 antibody (9G6) were performed in order to verify whether the enhanced cytotoxicity of our AAP system composed of three individual components (i.e., two recognition parts and Dox) is caused indeed by the bivalent recognition, followed by Dox release. Anti-HER2 antibody (9G6) was selected because this antibody is known for almost no potent killing effect on its own compared with anti-HER2 antibody (N12).<sup>26</sup> Supporting Information Figure S8 reveals that the increased cytotoxicity induced by one or two of the three individual components is of little significance in comparison with that induced by AAP-HER2-Dox or of Dox alone, although it is important to note that the three negative controls of Dox-loaded anti-thrombin 29-mer aptamer conjugated with anti-HER2 antibody, Dox-loaded ssDNA1 conjugated with anti-HER2 antibody, and Dox-loaded anti-HER2 aptamer conjugated with anti-HER2 antibody (9G6) exhibit the similar cytotoxicity with that of Aptamer-Dox or Antibody-Dox,

presumably due to the enhanced killing effect caused by the presence of either anti-HER2 antibody or aptamer.

Taken together with the observation that the cytotoxicity of AAP-HER2-Dox was found to be approximately 6-fold higher than that of anti-HER2 antibody (N12 or 9G6) alone (Supporting Information Figures S6 and S8), our results demonstrate that the drug-loaded AAP generates increased cytotoxicity to HER2-overexpressed human cells than each component in a cell- and dose-dependent manner, although recognition part-dependent toxicity of AAP-HER2-Dox needs to be further investigated in more detail. The results may reflect a difference in the drug uptake mechanism and/or the therapeutic antibody efficacy among Antibody-Dox, Aptamer-Dox, and Dox.

In addition, fluorescence microscopy was used, as depicted in Figure 4 and Supporting Information Figure S9, to evaluate the

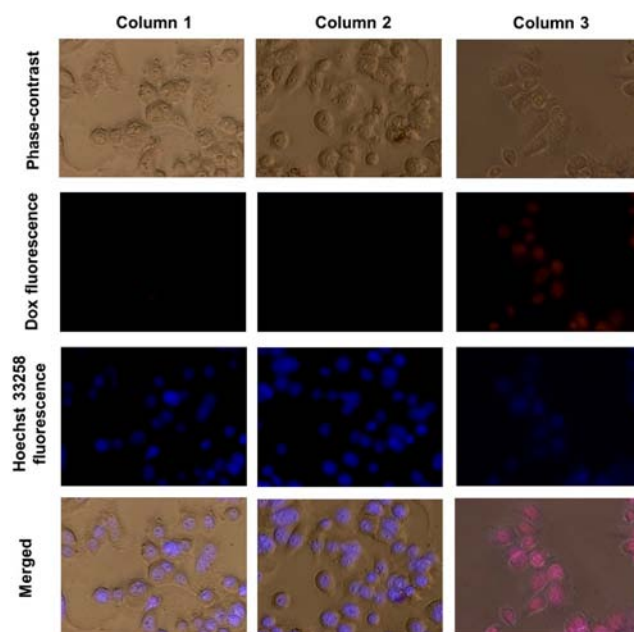


**Figure 4.** Dox release in SK-BR-3 cells when dosed with 100 nM (in terms of Dox) of Aptamer-Dox (column 1), Antibody-Dox (column 2), and AAP-HER2-Dox (column 3). The nuclei were stained by Hoechst 33258 and the images were taken after 4 h incubation. The results demonstrate that AAP-HER2-Dox constructed by conjugation of the antibody with the drug-loaded aptamer might effectively improve the affinities of the resulting AAP system for its target molecule and the drug-loaded AAP system could possibly serve as a platform for targeted DDS against many malignancies, which are notably consistent with the results shown in Figure 3.

intracellular uptake of Dox based on the fluorescence emitted by the drug. The results that AAP-HER2-Dox was effectively taken up by the cells suggest that the aptamer part of the complex possibly retained HER2-binding capability while carrying the drug within its DNA structure and that AAP-HER2-Dox could be used as a tumor-targeted DDS. It is interesting to note that the complex mostly stained the nuclei in HER2-overexpressed SK-BR-3 breast cancer cells (Figure 4), resulting in the lower IC<sub>50</sub> value observed.

## CONCLUSION

In summary, we developed a novel AAP system in this study. The AAP system, like antibody or aptamer dimerization from

other findings published recently, effectively improves the affinity with sustained or possibly higher specificity for its target molecule, and the drug-loaded AAP system may further serve as a platform for targeted DDS against many malignancies.

## ■ EXPERIMENTAL PROCEDURES

**Chemicals.** Reagents were obtained from commercial suppliers and were used without further purification, and double-distilled deionized water was used for all experiments. Antithrombin aptamers (15-mer DNA of 5'-H<sub>2</sub>N-(CH<sub>2</sub>)<sub>6</sub>-GGTTG GTGTG GTTGG-3' and 29-mer DNA of 5'-H<sub>2</sub>N-(CH<sub>2</sub>)<sub>6</sub>-AGTCC GTGGT AGGGC AGGTT GGGGT GACT-3'), anti-human epidermal growth factor 2 (HER2) aptamer (5'-H<sub>2</sub>N-(CH<sub>2</sub>)<sub>6</sub>-AACCG CCCAA ATCCC TAAGA GTCTG CACTT GTCAT TTTGT ATATG TATTT GGTTC TTGGC TCTCA CAGAC AACT ACACA CGCAC A-3') and single-stranded DNA 1 (ssDNA1, 5'-TGCAG CTCAT CA-3', a scrambled DNA sequence as the negative control) were obtained from Bioneer (Daejeon, Korea). HER2 epitope peptide (I-N-C-T-H-S-C-V-D-L-D-D-K-G-C-P-A-E-Q-R) was purchased from Peptron (Daejeon, Korea).<sup>25</sup> UV absorbance was measured using Agilent 8453 UV-visible spectrophotometer, and fluorescence spectra were recorded using a Synergy Mx spectrofluorophotometer (BioTek). All experiments were performed in triplicate.

**Conjugation of Anti-Thrombin DNA Aptamer with Anti-Thrombin Antibody (AAP-15 and AAP-29).** Sulfo-succinimidyl 4-(*N*-maleimidomethyl)cyclohexane-1-carboxylate (sulfo-SMCC, Sigma) was used in order to conjugate amine-functionalized DNA with the thiol-functionalized antibody by adapting the literature procedures.<sup>7,8</sup> In brief, amine-functionalized 15-mer DNA for AAP-15 or 29-mer DNA for AAP-29 (1.5 nmol) was maleimide-activated by incubation with sulfo-SMCC at a molar ratio of 1:10 (DNA:sulfo-SMCC) for 3 h at room temperature. Excess sulfo-SMCC was removed by centrifugation using an Amicon filter (Millipore) with a molecular weight cutoff of 3K Da. The resulting DNA was then used to be conjugated with *N*-succinimidyl-*S*-acetylthioacetate (SATA, ProteoChem)-functionalized anti-thrombin antibody, as follows.

SATA was conjugated with anti-thrombin antibody (F-1, Santa Cruz Biotech). According to the manufacturer's manual, the antibody (300 pmol) was incubated with SATA at a molar ratio of 1:10 (antibody:SATA) in the reaction buffer (0.1 M sodium phosphate, 0.15 M NaCl, 0.01 M EDTA, pH 7.2) for 2 h at room temperature, followed by addition of deacetylation solution (0.5 M NH<sub>2</sub>OH, 0.1 M sodium phosphate, 0.01 M EDTA, pH 7.2). After 2 h incubation at room temperature, excess SATA was removed by centrifugation using a microcon filter (Sartorius) with a molecular weight cutoff of 30K Da. The resulting antibody was reacted with the above maleimide-activated DNA in PBS solution (pH 7.4), followed by overnight reaction at room temperature for covalent bond formation and by removing unreacted DNA using a microcon filter (Sartorius) with a molecular weight cutoff of 30K Da.

FAM-labeled thrombin was prepared by 3 h reaction of thrombin (2 nmol, Enzyme Research Lab.) directly with NHS-activated FAM (Anaspec) at room temperature, followed by removing NHS-activated FAM using a microcon filter with a molecular weight cutoff of 30K Da. FAM-labeled bovine serum albumin (BSA) was also prepared in a similar fashion, except for using an Amicon filter with a molecular weight cutoff of 3K Da.

**Dialysis Experiments for Measurement of Dissociation Constants between Thrombin and AAP-15 or AAP-29.** For this purpose, the antibody-aptamer heterodimer solution contained in the dialysis caging (cutoff MW 50 000) was equilibrated against a solution containing the FAM-labeled thrombin or bovine serum albumin (BSA) (50 mM Tris-HCl buffer containing 140 mM NaCl, 1 mM MgCl<sub>2</sub>, 1 mM CaCl<sub>2</sub>, and 5 mM KCl, pH 7.4). Commercially available dialysis casings (Float-A-Lyzer G2 Dialysis Cassettes, Spectrum Lab) were used to minimize concentration changes due to osmotic pressure. By the fluorescence intensity measurement of the concentrations of the FAM-labeled proteins inside and outside the dialysis caging after equilibrium was reached, the amount of the FAM-labeled thrombin or BSA bound to the AAP was calculated. The *K<sub>d</sub>* value of the designed AAPs were calculated using OriginLab (OriginLab Corp.) or SigmaPlot (Systat Software), according to the literature.<sup>12</sup>

**Preparation of AAPs for Human Epidermal Growth Factor 2 (AAP-HER2).** AAP-HER2 was prepared similarly with AAPs for thrombin, as described above. Briefly, amine-functionalized DNA (1.0 nmol) was maleimide-activated by incubation with sulfo-SMCC at a molar ratio of 1:10 (DNA:sulfo-SMCC) for 3 h at room temperature. Excess sulfo-SMCC was removed by centrifugation using an Amicon filter with a molecular weight cutoff of 3K Da. The resulting DNA was then used to be conjugated with SATA-functionalized anti-HER2 antibody, as follows.

SATA was conjugated with anti-HER2 monoclonal antibody (N12, Thermo). According to the manufacturer's manual, the antibody (200 pmol) was incubated with SATA at a molar ratio of 1:10 (antibody:SATA) in the reaction buffer for 2 h at room temperature, followed by addition of deacetylation solution. After 2 h incubation at room temperature, excess SATA was removed by centrifugation using a microcon filter with a molecular weight cutoff of 30K Da. The resulting antibody was reacted with the above maleimide-activated DNA in PBS solution (pH 7.4), followed by overnight reaction at room temperature for covalent bond formation and by removing unreacted DNA using a microcon filter with a molecular weight cutoff of 30K Da.

Preparation of doxorubicin (Dox)-loaded AAP-HER2 (AAP-HER2-Dox), Dox-loaded anti-HER2 aptamer (Aptamer-Dox), and Dox-mixed anti-HER2 antibody (Antibody-Dox). Dox was loaded into the DNA structure of the aptamer or mixed with anti-HER2 antibody by adapting the literature protocols.<sup>25</sup> Without preheating the aptamer-containing materials, a fixed concentration of aptamer (50 pmol) was incubated for 3 h at room temperature with various concentrations of Dox, at Dox/aptamer molar ratios of 0.5, 1, 4, 10, 50, and 100, respectively. For comparison, a fixed concentration of antibody (10 pmol) was incubated for 3 h at room temperature with various concentrations of Dox, at Dox/antibody molar ratios of 1, 2, and 4, respectively. The fluorescence spectrum of doxorubicin was examined in 96-well black plate by a Synergy Mx spectrofluorophotometer.

In a similar fashion, anti-HER2 monoclonal antibody (N12) was covalently linked to anti-thrombin 29-mer aptamer and ssDNA1, respectively, as negative controls. Anti-HER2 monoclonal antibody (9G6, Thermo) was conjugated with anti-HER2 aptamer, to be used as another negative control, because this antibody is known for almost no potent killing effect on its own compared with anti-HER2 antibody (N12).<sup>26</sup>

**Evaluation of Dox Release from Dox-Loaded anti-HER2 Aptamer in the Presence of HER2 Epitope Peptide.** Various concentrations of HER2 epitope solutions were mixed with a fixed concentration (250 nM) of anti-HER2 aptamer at fixed molar ratios of Dox of 10, and various concentrations of Dox-loaded anti-HER2 aptamer solutions at fixed molar ratios of Dox of 10 were mixed with a fixed concentration (250 nM) of HER2 epitope peptide. The fluorescence spectrum of doxorubicin was examined in 96-well black plate after 0.5 h and 6 h incubation by a Synergy Mx spectrofluorophotometer.

**Cell Culture, Cell Viability Assay, And Fluorescence Imaging.** SK-BR-3, MDA-MB-453, and MCF-7 human breast cancer cells were obtained from American Type Culture Collection and were maintained in tissue culture plates at 37 °C in an atmosphere of 5% CO<sub>2</sub> in RPMI-1640 media, supplemented with 2 mM L-glutamine, 10% fetal bovine serum, 100 IU/mL penicillin, and 0.1 mg/mL streptomycin. In order to keep cells in log phase, the cultures were re-fed with fresh media two or three times/week.

Cell viability was assessed using the standard 3-(4,5-dimethylthiazol-2-yl)-2,5-diphenyltetrazolium bromide (MTT) reduction assay according to the literature.<sup>27</sup> In brief, exponentially growing cells were seeded in 96-well flat-bottomed microplates (200  $\mu$ L/well) at a density of  $5 \times 10^3$  cell per well, and after 24 h incubation at 37 °C, followed by exposure for 24 h to various concentrations of AAP-HER2-Dox, Antibody-Dox, Aptamer-Dox, Dox, anti-HER2 antibody, and anti-HER2 aptamer, respectively. For each concentration at least 8 wells were used. After incubation, 10  $\mu$ L of MTT solution (5 mg/mL in PBS) was added and the microplates were further incubated for 4 h at 37 °C. The quantity of formazan product obtained was determined at 570 nm. The cell survival fractions were calculated as percentage of the untreated control. The experimental data were transformed to dose-response curves using nonlinear regression analysis (SigmaPlot) to obtain the theoretical curves and to calculate the corresponding IC<sub>50</sub> values. Fluorescence microscopy was performed with an Axio Observer Z1 inverted microscope (Carl Zeiss Inc., USA).

## ■ ASSOCIATED CONTENT

### ■ Supporting Information

Additional information as noted in the text (Figures S1–S9). This material is available free of charge via the Internet at <http://pubs.acs.org>.

## ■ AUTHOR INFORMATION

### Corresponding Author

\*E-mail: [sshah@khu.ac.kr](mailto:sshah@khu.ac.kr).

### Notes

The authors declare no competing financial interest.

## ■ ACKNOWLEDGMENTS

This work was supported by Basic Science Program through the National Research Foundation of Korea (KRF) funded by the Ministry of Science, ICT and Future Planning (MSIP) (2011-0021956), and by the Ministry of Education (MOE) (2012-001680).

## ■ REFERENCES

- (1) Adams, G. P., and Schier, R. (1999) Generating improved single-chain Fv molecules for tumor targeting. *J. Immunol. Methods* 231, 249–260.
- (2) Viti, F., Tarli, L., Giovannoni, L., Zardi, L., and Neri, D. (1999) Increased binding affinity and valence of recombinant antibody fragments lead to improved targeting of tumoral angiogenesis. *Cancer Res.* 59, 347–352.
- (3) Neri, D., Momo, M., Prospero, T., and Winter, G. (1995) High-affinity antigen binding by chelating recombinant antibodies (BRABs). *J. Mol. Biol.* 246, 367–373.
- (4) Tuerk, C., and Gold, L. (1990) Systematic evolution of ligands by exponential enrichment: RNA ligands to bacteriophage T4 DNA polymerase. *Science* 249, 505–510.
- (5) Nimjee, S. M., Rusconi, C. P., and Sullenger, B. A. (2005) Aptamers: an emerging class of therapeutics. *Annu. Rev. Med.* 56, 555–583.
- (6) Shin, S., Kim, I. H., Kang, W., Yang, J. K., and Hah, S. S. (2010) An alternative to Western blot analysis using RNA aptamer-functionalized quantum dots. *Bioorg. Med. Chem. Lett.* 20, 3322–3325.
- (7) Lee, G. H., and Hah, S. S. (2012) Coomassie blue is sufficient for specific protein detection of aptamer-conjugated chips. *Bioorg. Med. Chem. Lett.* 22, 1520–1522.
- (8) Kim, J., Lee, G. H., Jung, W., and Hah, S. S. (2013) Selective and quantitative cell detection based both on aptamers and the conventional cell-staining methods. *Biosens. Bioelectron.* 43, 362–365.
- (9) Lee, E. J., Lim, H. K., Cho, Y. S., and Hah, S. S. (2013) Peptide nucleic acids are an additional class of aptamers. *RSC Adv.* 3, 5828–5831.
- (10) Ueyama, H., Takagi, M., and Takenaka, S. (2002) A novel potassium sensing in aqueous media with a synthetic oligonucleotide derivative. Fluorescence resonance energy transfer associated with Guanine quartet-potassium ion complex formation. *J. Am. Chem. Soc.* 124, 14286–14287.
- (11) Wang, L., Liu, X., Hu, X., Song, S., and Fan, C. (2006) Unmodified gold nanoparticles as a colorimetric probe for potassium DNA aptamers. *Chem. Commun.* 36, 3780–3782.
- (12) Kim, J., Kim, M. Y., Kim, H. S., and Hah, S. S. (2011) Binding of uranyl ion by a DNA aptamer attached to a solid support. *Bioorg. Med. Chem. Lett.* 21, 4020–4022.
- (13) Sankaran, N. B., Nishizawa, S., Seino, T., Yoshimoto, K., and Teramae, N. (2006) Abasic-site-containing oligonucleotides as aptamers for riboflavin. *Angew. Chem., Int. Ed.* 45, 1563–1568.
- (14) Liu, J., and Lu, Y. (2006) Fast colorimetric sensing of adenosine and cocaine based on a general sensor design involving aptamers and nanoparticles. *Angew. Chem., Int. Ed.* 45, 90–94.
- (15) Fang, X., and Tan, W. (2010) Aptamers generated from cell-SELEX for molecular medicine: A chemical biology approach. *Acc. Chem. Res.* 43, 48–57.
- (16) Kim, Y., Cao, Z., and Tan, W. (2008) Molecular assembly for high-performance bivalent nucleic acid inhibitor. *Proc. Natl. Acad. Sci. U.S.A.* 105, S664–S669.
- (17) Hasegawa, H., Taira, K., Sode, K., and Ikebukuro, K. (2008) Improvement of aptamer affinity by dimerization. *Sensors* 8, 1090–1098.
- (18) Holland, C. A., Henry, A. T., Whinna, H. C., and Church, F. C. (2000) Effect of oligonucleotide thrombin aptamer on thrombin inhibition by heparin cofactor II and anti-thrombin. *FEBS Lett.* 484, 87–91.
- (19) Bock, L. C., Griffin, L. C., Latham, J. A., Vermaas, E. H., and Toole, J. J. (1992) Selection of single-stranded DNA molecules that bind and inhibit human thrombin. *Nature* 355, 564–566.
- (20) Macaya, R. F., Schultze, P., Smith, F. W., Roe, J. A., and Feigon, J. (1993) Thrombin-binding DNA aptamer forms a unimolecular quadruplex structure in solution. *Proc. Natl. Acad. Sci. U.S.A.* 90, 3745–3749.
- (21) Smirnov, I., and Shafer, R. H. (2000) Effect of loop sequence and size on DNA aptamer stability. *Biochemistry* 39, 1462–1468.

(22) Tennico, Y. H., Hutanu, D., Koesdjojo, M. T., Bartel, C. M., and Remcho, V. T. (2010) On-chip aptamer-based sandwich assay for thrombin detection employing magnetic beads and quantum dots. *Anal. Chem.* 82, 5591–5597.

(23) Elg, S., and Deinum, J. (2002) The interaction between captured human thrombin and antithrombin studied by surface plasmon resonance, and the effect of melagatran. *Spectroscopy* 16, 257–270.

(24) Hermeling, S., Crommelin, D. J. A., Schellekens, H., and Jiskoot, W. (2004) Structure-immunogenicity relationships of therapeutic proteins. *Pharm. Res.* 21, 897–903.

(25) Liu, Z., Duan, J. H., Song, Y. M., Ma, J., Wang, F. D., Lu, X., and Yang, X. D. (2012) Novel HER2 aptamer selectively delivers cytotoxic drug to HER2-positive breast cancer cells in vitro. *J. Translational Med.* 10, 148 DOI: 10.1186/1479-5876-10-148.

(26) Yip, Y. L., Smith, G., Koch, J., Duebel, S., and Ward, R. L. (2001) Identification of epitope regions recognized by tumor inhibitory and stimulatory anti-ErbB-2 monoclonal antibodies: Implications for vaccine design. *J. Immunol.* 166, 5271–5278.

(27) Mosmann, T. (1983) Rapid colorimetric assay for cellular growth and survival: application to proliferation and cytotoxicity assays. *J. Immunol. Methods* 65, 55–63.